

# The Ternary Complex Model

## Its Properties and Application to Ligand Interactions with the D<sub>2</sub>-Dopamine Receptor of the Anterior Pituitary Gland

KEITH A. WREGGETT AND ANDRÉ DE LÉAN

*Institut de Recherches Cliniques de Montréal, Montréal, Québec, H2W 1R7 Canada*

Received December 20, 1983; Accepted June 7, 1984

### SUMMARY

Agonists and antagonists interact with the pituitary D<sub>2</sub>-dopamine receptor in a complex fashion that has been accounted for by proposing that the receptor exists in two interconvertible affinity states [De Lean *et al.*, *Mol. Pharmacol.* 22:290-297 (1982)]. These two states appear to be modulated by guanine nucleotides such that the state existing in the presence of excess guanine nucleotide has low affinity for agonists and high affinity for antagonists. These observations, together with several lines of evidence from other laboratories, have suggested the interaction of the receptor with a guanine nucleotide-binding protein and a model describing the reversible interaction of the receptor (*R*) with an additional membrane component (*X*) was studied [De Lean *et al.*, *J. Biol. Chem.* 255:7108-7117 (1980)]. Several properties of this ternary complex model are presented and discussed in terms of the interpretation of the analysis of simulated binding data using the mass-action model. Computer modeling of experimental binding data obtained from membrane homogenates of bovine anterior pituitary glands indicated that a ternary complex model will fit only under conditions where, in the absence of any ligand, there is a tight interaction or "precoupling" of *R* with *X*, with the latter being in stoichiometrically limiting amounts; antagonists and guanine nucleotides would tend to destabilize this interaction, whereas agonists would serve to stabilize the coupled form. These results, for a receptor system that inhibits adenylate cyclase activity, are notably different from those observed for the *beta*-adrenergic receptor, which stimulates the enzyme and may be a reflection of differences in the molecular mechanisms of the interaction of the two receptor systems with their ligands and their effector. Some features of the model are not compatible with the experimental data and have indicated the need to consider extensions of the model, in light of recent advancements in our understanding of these regulatory components. Our results stress the importance of verifying the properties of proposed models and of cautiously testing these proposed models by their direct application to experimental data.

### INTRODUCTION

The concept of pharmacological agonists and antagonists can be shown to extend down to the level of the receptor, where ligand-specific binding properties may be a reflection of early steps leading to the activation of a cellular response. In several systems where guanine nucleotides have been shown to have an essential role in the mediation of hormone-stimulated biochemical responses, these purine derivatives have also been observed to decrease specifically the binding of agonists to their

receptor; the binding of antagonists, which do not produce a response, does not appear to be affected by guanine nucleotides.

We have previously described many of the binding properties of the D<sub>2</sub>-dopamine receptor in the porcine anterior pituitary gland (1), a system that appears to inhibit adenylate cyclase activity (2). These data were adequately described with a model based on independent classes of binding sites (Fig. 1), analyses indicating that in this system both agonists and antagonists discriminated two apparent binding sites existing in equal proportions. Guanine nucleotides appeared to promote interconversion between the two apparent binding sites; the apparent binding site predominating in the presence of excess guanine nucleotides had high affinity for an-

This work was supported by the Medical Research Council of Canada. Some aspects of this work were presented at the International Symposium on Catecholamines as Hormone Regulators, Indianapolis, Ind., September 12-14, 1983.

0026-895X/84/050214-14\$02.00/0

Copyright © 1984 by The American Society for Pharmacology and Experimental Therapeutics.

All rights of reproduction in any form reserved.

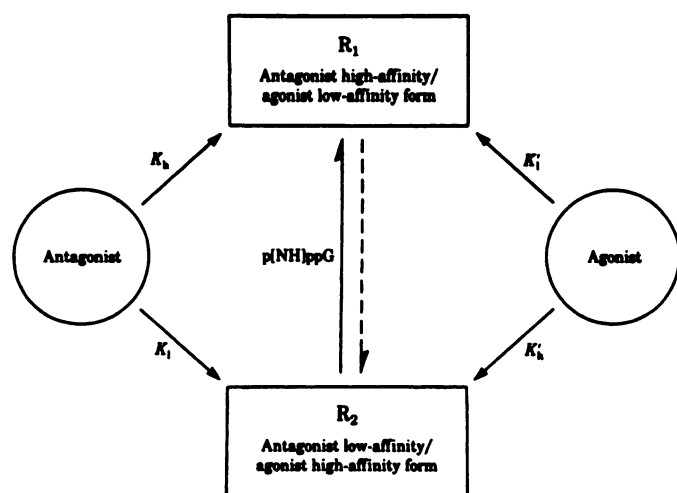


FIG. 1. Reciprocal model for interaction of agonists and antagonists with the  $D_2$ -dopamine receptor of the anterior pituitary gland

This model, based on independent classes of binding sites, was previously proposed by us (1) to describe the observed ligand-binding data and the modulatory effect of guanine nucleotides.

tagonists and low affinity for agonists. These observations were incompatible with the possibility of there existing two distinct, independent classes of binding sites. As a first approach we proposed, in analogy to our earlier studies of the  $\beta$ -adrenergic receptor of the frog erythrocyte (3, 4), that the  $D_2$ -dopamine receptor in the porcine anterior pituitary gland interacts with a guanine nucleotide-binding protein so that two interconvertible affinity states of the receptor are detected, each state having reciprocal affinity for dopaminergic agonists and antagonists (1). We also provided other evidence in support of the involvement of a guanine nucleotide-binding protein in the interaction of dopaminergic ligands with their receptor by demonstrating that agonist binding to the apparent high-affinity binding site was selectively decreased by low concentrations ( $<1$  mM) of NEM<sup>1</sup> and by moderate heat treatment (5). Both treatments have been demonstrated to inactivate selectively a guanine nucleotide-binding protein in several systems (6, 7).

Further evidence in support of an involvement of the pituitary dopamine receptor with a guanine nucleotide-binding protein comes from the recent demonstration that pretreatment of cultured rat pituitary cells with a *Bordetella pertussis* toxin, IAP, results in the elimination of dopamine inhibition of prolactin secretion (8), in analogy with other inhibitory receptor systems where IAP has been shown to modify specifically a guanine nucleotide-regulatory protein (9–11). It has also been recently demonstrated that the solubilized bovine pituitary dopamine receptor has an apparent higher molecular size when occupied by agonists than when occupied by antagonists (12)—an observation again consistent with the concept that agonists promote the interaction of the receptor with a distinct membrane component.

<sup>1</sup> The abbreviations used are: NEM, *N*-ethylmaleimide; IAP, islet-activating protein; ADTN, ( $\pm$ )-6,7-dihydroxy-1,2,3,4-tetrahydronaphthalene; Gpp(NH)p, guanylyl-5'-imidodiphosphate;  $K_{PNP}$ , equilibrium association constant of ligand in the presence of Gpp(NH)p; NPA, (–)-*N*-propylnorapomorphine.

When first proposed for and applied to the  $\beta$ -adrenergic receptor (4), the ternary complex model (Fig. 2) was the simplest and best available explanation to account for the characteristics of ligand binding data and for the apparent allosteric interaction between hormones and guanine nucleotides. Since that time, direct reference to this model has been made to account for similarly observed properties in other receptor systems (13–16). In these later studies the conclusions were based on data analysis using models predicated on independent classes of binding sites, in analogy to the results obtained from similar studies of the  $\beta$ -adrenergic receptor (3). Previously, however, there has been no detailed presentation of the properties of the ternary complex model, nor has the relevance of this model been tested further by applying it directly to another receptor system. As well, there has not been any direct study comparing the parameters of the ternary complex model with those using a model based on independent classes of binding sites.

In this study we have examined the theoretical properties of a ternary complex model, focusing on those which allow for discrimination of two apparent affinity states by both agonists and antagonists. This theoretical study, together with the direct application of this model to the ligand-binding data of the  $D_2$ -dopamine receptor, is presented and includes parallel analyses by equations based on independent classes of binding sites of binding data obtained from simulations of a ternary complex model.

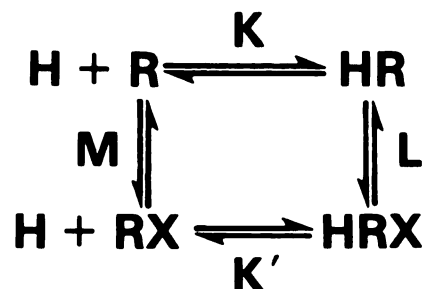


FIG. 2. Ternary complex model

This model, describing the reversible interaction of the receptor  $R$  with a regulatory component  $X$ , was previously proposed by us (4) to explain agonist-specific binding properties of the  $\beta$ -adrenergic receptor. Briefly stated, the model is described by four equilibrium reactions: two binding steps, common to all ligands ( $H$ ), involving either the free receptor,  $R$ , or the coupled receptor,  $RX$ , both reactions characterized by the equilibrium association constants  $K$  and  $K'$ , respectively; a transition step, characterized by the association constant  $L$ , describing the equilibrium between the ligand-bound receptor ( $HR$ ) and the ligand-bound, coupled receptor (ternary complex,  $HRX$ ); an equilibrium between  $R$  and  $RX$ , describing the interaction between the receptor and the regulatory component, characterized by the association constant  $M$ . Because of thermodynamic constraints, the affinity-ratio  $K'/K$  must equal the stability ratio  $L/M$ . Ligands with the property of  $L > M$  will serve to promote or stabilize the interaction between the receptor  $R$  and the regulatory component  $X$ , in the form of the ternary complex ( $HRX$ ), whereas ligands with the property of  $L < M$  will serve to destabilize this interaction. Thus, the characteristics of equilibrium binding data, which are a result of the interaction of the receptor  $R$  with the regulatory component  $X$ , will depend on the relative values of  $L/M$  for any ligand competing for the binding to the two forms of the receptor and on the relative stoichiometry of the receptor  $R$  and the regulatory component  $X$ .

## EXPERIMENTAL PROCEDURES

**Materials.** [ $^3\text{H}$ ]Spiperone (23–25 Ci/mmol) was purchased from New England Nuclear Corporation (Boston, Mass.). Drugs were obtained from the following sources: ADTN, Research Biochemicals, Inc. (Wayland, Md.); apomorphine, Sigma Chemical Company (St. Louis, Mo.); NPA, Sterling-Winthrop Research Institute (Rensselaer, N.Y.). All buffer reagents were purchased from either Fisher Scientific Company Ltd. (Montreal, Que.) or Sigma Chemical Company. Gpp(NH)p, as the sodium salt, was purchased from either Boehringer Mannheim (Dorval, Que.) or Sigma Chemical Company.

**Membrane preparation.** Membranes from steer anterior pituitary glands were prepared as published previously (1). Briefly stated, the anterior lobes were dissected within minutes of death, frozen on dry ice, and then stored at  $-70^\circ$ . Within 2 weeks, all tissue was prepared by homogenization in 25 mM Tris/5 mM  $\text{MgCl}_2$ /250 mM sucrose (Buffer A) using a glass-Teflon homogenizer, filtration through cheesecloth, and centrifugation of the supernatant at  $300 \times g$  for 10 min. A 10-ml aliquot of a 25 mM Tris/60% sucrose solution was layered under 25 ml of the resultant supernatant in 50-ml polycarbonate tubes that were then centrifuged for 30 min at  $30,000 \times g$ . The interface fraction was collected and washed once by resuspension in Buffer A and centrifugation for 30 min at  $30,000 \times g$ . This pellet was resuspended in Buffer A (2 ml of buffer per gram of original tissue), frozen in liquid nitrogen, and stored at  $-70^\circ$  until used. All preparation steps were performed at  $4^\circ$  and all buffers were pH 7.4 at  $4^\circ$ .

**Radioligand-binding assay.** Membranes were thawed and diluted in an assay buffer consisting of 50 mM Tris/100 mM NaCl/6 mM  $\text{MgCl}_2$ /1 mM EDTA/0.1% ascorbic acid/10  $\mu\text{M}$  pargyline (pH 7.4 at  $25^\circ$ ) (Buffer B). These membranes were then incubated with [ $^3\text{H}$ ]spiperone in the presence of various compounds in a total volume of 2 ml of Buffer B for 45 min at  $25^\circ$  in glass tubes ( $12 \times 75$  mm). Total protein per tube was 100–200  $\mu\text{g}$ . The reaction was initiated by addition of the membranes and terminated by vacuum filtration through GF/B glass-fiber filters followed by a total of nine 3-ml washes with ice-cold buffer (50 mM Tris/6 mM  $\text{MgCl}_2$ , pH 7.4 at  $4^\circ$ ). All measurements were made in duplicate. Bound radioactivity trapped on the filters was determined by liquid scintillation spectrophotometry. Nonspecific binding was defined by using 5  $\mu\text{M}$  (+)-butaclamol.

**Data analysis.** See Appendix.

## RESULTS

## Simulations Using the Ternary Complex Model

Simulations based on the ternary complex model were performed to describe the general properties of the model; consideration was given to those predicted properties which would be most testable of the model by direct experimentation in a real system. In all presentations, analysis of these simulated data with the mass-action model was performed to attempt to identify any relationship between the respective parameters of the two models.

## Saturation Curves

Simulations of saturation curves indicated that under most conditions the curves could be described by a simple rectangular hyperbola (slope factor = 1), consistent with only a single class of apparent binding sites. Such was the case when the ligand had equal affinity for both forms of the receptor,  $R$  and  $RX$  (curve *a*, Fig. 3A and B) or in the absence of the regulatory component  $X$  (curve *a*, Fig. 3C; curve *e*, Fig. 4). Deviation from this property was observed when the radioligand had differing affinity for the two forms of the receptor (Fig. 3A and B), this effect being maximal when the amounts of the receptor

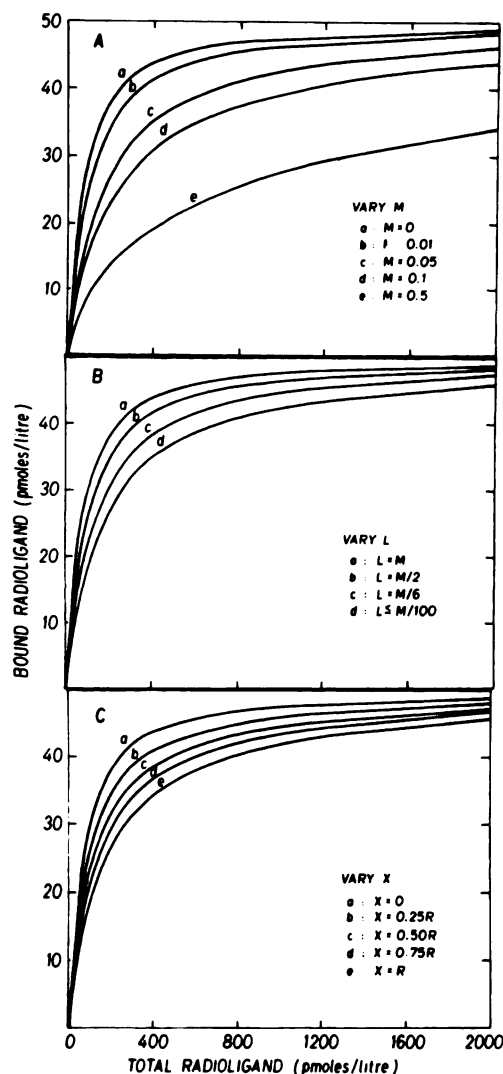


FIG. 3. Simulation of receptor saturation curves using the general form of the ternary complex model

All curves were generated considering a radioligand that was unable to stabilize the ternary complex  $HRX$  ( $L/M < 1$ ). A. Increasing the interaction of the receptor  $R$  with the regulatory component  $X$  (increasing  $M$ ) resulted in a "shallower" curve (slope factor  $< 1$ ) as a larger fraction of the receptor was in the "precoupled" form  $RX$  for which the radioligand had lower affinity. B. In the case of a moderate interaction of the receptor  $R$  and the regulatory component  $X$  ( $M = 6 \times 10^{10} \text{ M}^{-1}$ ; about 60% of the receptor was in the "precoupled" form  $RX$ ), the preference of the radioligand for the free form of the receptor  $R$  was increased by decreasing the value of  $L$ . A limit in the slope of the saturation curve was reached where  $L/M \ll 1$ . In this limit, the radioligand would be binding predominantly to the free form of the receptor  $R$ , and it would be impossible to obtain an estimate of the affinity of the radioligand for the coupled form of the receptor  $RX$ . C. Under limiting conditions where  $L/M \ll 1$ , the saturation curve attained a minimum slope when there were stoichiometrically similar amounts of the receptor  $R$  and the regulatory component  $X$ .

and the regulatory component were the same (Fig. 3C). Analysis of simulated saturation curves having increasing amounts of the regulatory component using the mass-action model indicated increasing amounts of an apparent low-affinity binding site ( $R_L$ ) with no change in the association constants of the two apparent binding sites



(data not shown). The simulations indicated that, if the ligand bound predominately to the free form of the receptor  $R$ , it was acting to destabilize any pre-existing coupled receptor ( $RX$ ). In this case the "shallow" saturation curve would be a reflection of this gradual shift in the equilibrium from  $RX$  to  $R$  by increasing concentrations of the ligand and would not be the result of interaction of the ligand with a low-affinity binding site (Table 1).

### Competition Curves

Effect of varying the amount of the regulatory component. Several experimental approaches are available either to reduce the amount of or to inactivate the regulatory component in the membrane. The properties of the competition curve for any ligand will depend to a large extent on the stoichiometry between the total amount of the receptor  $R$  and that of the regulatory component  $X$ . In the absence of the regulatory component  $X$ , the curve could be explained by a single class of binding sites (curve  $e$ , Fig. 4), but with the introduction of the regulatory component  $X$  the curve became progressively "shallow" (slope factor  $< 1$ ), results indicating increasing amounts of an apparent high-affinity binding site (Fig. 4; Table 2).

*Different competing ligands while varying the amount of the regulatory component.* Under the conditions described in the previous section, when the amounts of the receptor  $R$  and the regulatory component  $X$  were comparable ( $X/R = 1$ ), the amount of the apparent high-affinity binding site ( $R_H$ ) determined from competition data with the mass-action model would vary with different competing ligands. Under these conditions, the proportion of the apparent high-affinity binding site  $R_H$ , determined with the mass-action model, is positively

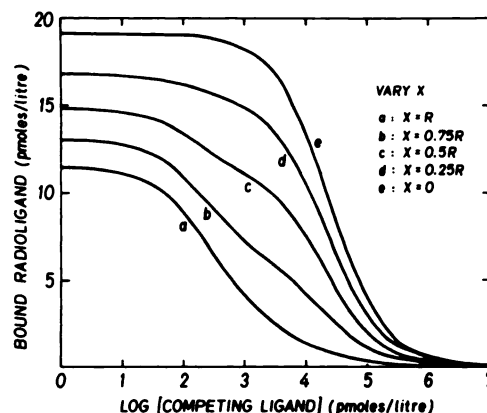


FIG. 4. Simulation of competition curves using the general form of the ternary complex model, varying the amount of total regulatory component  $X$

Competition curves were generated by considering a system with a moderate amount of spontaneous interaction between the receptor  $R$  and the regulatory component  $X$  ( $M = 6 \times 10^{10} \text{ M}^{-1}$ ), resulting in about 60% of the total receptor concentration being "precoupled" in the form of  $RX$  in the absence of any ligand. The radioligand had preferential affinity for the free form of the receptor  $R$  ( $L/M \ll 1$ ), and the competing ligand had higher affinity for the coupled form of the receptor  $RX$  ( $L/M > 1$ ). Introduction of the regulatory component  $X$  to the system leads to substantially more of the total receptor concentration in the form ( $RX$ ) having low affinity for the radioligand and high affinity for the competing ligand (Table 2). This results in the observed changes in the shape of the competition curve, including the lowering of the initial level of binding of the radioligand in the absence of any competing ligand (see also Fig. 3C).

correlated with the maximal amount of the ternary complex  $HRX$  formed in the presence of the competing ligand. As described previously (4, 16), the ternary complex model also predicts that, in the analysis of competition data with the mass-action model, there is a positive correlation of the proportion of the apparent high-affinity binding site  $R_H$  and the ability of the competing ligand to discriminate the two apparent binding sites (i.e.,  $\%R_H$  and  $K_H/K_L$  are positively correlated).

However, in cases where the amount of the regulatory component  $X$  was stoichiometrically limiting ( $X/R = 0.25\text{--}0.75$ ), the amount of total ternary complex  $HRX$  that could be formed in the presence of the ligand depended on the concentration of total regulatory component  $X$  (Fig. 5A; Table 3). Analysis with the mass-action model indicated that for all competing ligands having higher affinity for the coupled form of the receptor ( $L/M > 1$ ) the ratio of the apparent association constants ( $K_H/K_L$ ) was positively correlated with the change in  $L/M$  (Table 3; Fig. 6).

Simulations also predicted that, under normal experimental conditions, a ligand having higher affinity for the free form of the receptor ( $L/M < 1$ ) would apparently exhibit a form of "noncompetitive" competition (decreases in both apparent affinity and binding capacity) in the presence of another ligand having higher affinity for the coupled form of the receptor ( $L/M > 1$ ), since these two ligands would effectively be binding to distinct, but interconvertible, forms of the receptor (data not shown).

*Correct use of radioligand binding constants.* Using the

TABLE 1

Parameter estimates from mass-action modeling of simulated saturation curves in the case where the amount of the regulatory component was varied

Data were simulated\* as described in Fig. 3C but with the introduction of "experimental noise" (see Appendix). Analysis with the mass-action model indicated that in the absence of the regulatory component  $X$  ( $X/R = 0$ ) the data were consistent with a single class of binding sites having an association constant ( $K_H$ ) identical with the value of  $K$  (association constant of the ligand for the free form of the receptor  $R$ ; see Fig. 2) used to simulate the data. Introduction of the regulatory component  $X$  in the simulations resulted in the data being best described with two apparent binding sites, the proportion of the apparent high-affinity binding site ( $\%R_H$ ) decreasing accordingly. The value of the association constant of the low-affinity binding site ( $K_L$ ) was dependent upon the ability of the ligand to discriminate the two forms of the receptor (i.e., on the ratio of  $L/M$ ; see Fig. 2).

$X/R$	$K_H$ $\text{M}^{-1}$	$K_L$ $\text{M}^{-1}$	$\%R_H$
0.00	$1.98 \pm 0.01 \times 10^{10}$	—	100
0.25	$1.98 \pm 0.01 \times 10^{10}$	$4.4 \pm 0.1 \times 10^9$	$79 \pm 2$
0.50	$1.98 \pm 0.01 \times 10^{10}$	$4.4 \pm 0.1 \times 10^9$	$57 \pm 2$
0.75	$1.98 \pm 0.01 \times 10^{10}$	$4.4 \pm 0.1 \times 10^9$	$40.0 \pm 0.1$
1.00	$1.98 \pm 0.01 \times 10^{10}$	$4.4 \pm 0.1 \times 10^9$	$28.7 \pm 0.7$

\* Simulated parameters were  $R = 50 \text{ pM}$ ;  $K = 2 \times 10^{10} \text{ M}^{-1}$ ;  $L = 0 \text{ M}^{-1}$ ;  $M = 6 \times 10^{10} \text{ M}^{-1}$ .

TABLE 2

Parameter estimates from mass-action modeling of simulated competition curves in the case where the amount of the regulatory component was varied

Data were simulated<sup>a</sup> as described in Fig. 4 but with the introduction of "experimental noise" (see Appendix). Analysis with the mass-action model was performed assuming association constants of the radioligand as determined from analysis of simulated saturation curves (see Table 1). With increasing amounts of the regulatory component  $X$  ( $X/R > 0$ ), there was an increase in the proportion of an apparent high-affinity binding site ( $\%R_H$ ). In the absence of the regulatory component ( $X/R = 0$ ), the single association constant observed ( $K_L$ ) was identical with  $K$  (association constant of the competing ligand for the free form of the receptor; see Fig. 2). The value of  $K_L$  was significantly different from  $K$  when the amounts of the regulatory component and the receptor were similar ( $X/R = 1$ ;  $p < 0.001$ ). With limiting amounts of the regulatory component, the value of  $\%R_H$  was significantly underestimated if the analysis was conducted assuming that the radioligand did not discriminate the two forms of the receptor (parameter estimates in parentheses).

$X/R$	$K_H$ $M^{-1}$	$K_L$ $M^{-1}$	$\%R_H$
0.00	—	$1.0 \pm 0.1 \times 10^8$	0
0.25	$1.3 \pm 0.9 \times 10^{10}$ ( $2 \pm 1 \times 10^{10}$ )	$1.0 \pm 0.1 \times 10^8$ ( $9.8 \pm 0.2 \times 10^7$ )	$26 \pm 1$ ( $13 \pm 1$ )
0.50	$8 \pm 2 \times 10^9$ ( $1.1 \pm 0.3 \times 10^{10}$ )	$1.1 \pm 0.1 \times 10^8$ ( $9.8 \pm 0.1 \times 10^7$ )	$49 \pm 1$ ( $30 \pm 2$ )
0.75	$6.0 \pm 0.6 \times 10^9$ ( $7 \pm 1 \times 10^9$ )	$1.3 \pm 0.1 \times 10^8$ ( $1.0 \pm 0.1 \times 10^8$ )	$70 \pm 1$ ( $60 \pm 1$ )
1.00	$1.0 \pm 0.1 \times 10^{10}$ ( $7.7 \pm 0.2 \times 10^9$ )	$6.1 \pm 0.2 \times 10^8$ ( $2.6 \pm 0.1 \times 10^8$ )	$81 \pm 1$ ( $82 \pm 1$ )

<sup>a</sup> Simulated values were  $K = 1 \times 10^8 M^{-1}$ ,  $L = 5 \times 10^{12} M^{-1}$  for the competing ligand;  $K = 2 \times 10^{10} M^{-1}$ ,  $L = 0 M^{-1}$  for the radioligand;  $M = 6 \times 10^{10} M^{-1}$ ;  $R = 50$  pM.

mass-action model as a tool to attempt to quantify parameters pertaining to the ternary complex model can often lead one astray, as there is no direct relationship between these two models. This problem is especially prevalent if the radioligand is able to discriminate the two forms of the receptor, for then both  $\%R_H$  and the value of  $K_H/K_L$  will be miscalculated if the analysis was conducted assuming that the radioligand was nondiscriminating (Fig. 5B; Table 4; see also all estimates in parentheses given in Tables 2, 3, and 5, where the analysis was conducted under this assumption). This error in estimation of the proportion of the apparent high-affinity binding site  $R_H$  or of the selectivity ratio  $K_H/K_L$  can be avoided by utilizing in the analysis the correct apparent association constants for the radioligand, the most accurate results being obtained using the reciprocal model outlined in Fig. 1.

**Destabilization of receptor/regulatory component interaction.** It was of interest to study the effect of decreasing the degree of interaction between the receptor  $R$  and the regulatory component  $X$  in what could be proposed as a working model for the effect of guanine nucleotides on ligand binding properties. It was considered that any factor acting to decrease the spontaneous interaction of the receptor  $R$  and the regulatory component  $X$  (de-

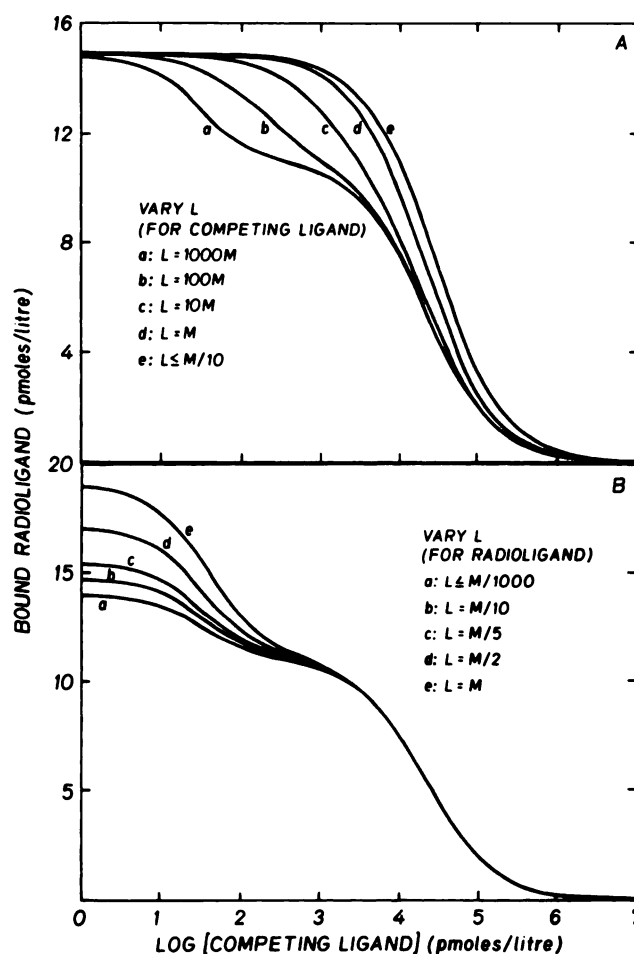


FIG. 5. Simulation of competition curves with various competing ligands using the general form of the ternary complex model

The amount of total regulatory component  $X$  was less than that of the receptor  $R$  ( $R = 2X$ ). A. Competition curves by various ligands were obtained by varying their ability to stabilize the interaction of the receptor  $R$  and the regulatory component  $X$  in the form  $HRX$  (varying  $L$ ). The radioligand had preferential affinity for the free form of the receptor ( $L/M \ll 1$ ), and there was a moderate amount of spontaneous interaction of the receptor  $R$  and the regulatory component  $X$ . The inflection point of these complex curves was the same for all competing ligands that could stabilize the ternary complex  $HRX$  ( $L/M > 1$ ). B. The shape of the competition curve depended upon the ability of the radioligand to discriminate the two forms of the receptor; the competing ligand had higher affinity for the coupled form of the receptor ( $L/M > 1$ ). As the preference of the radioligand for the free form of the receptor  $R$  was increased ( $L/M \rightarrow 0$ ), there was less an apparent high-affinity binding site recognized by the competing ligand (see also Table 4). Competition curves more effectively revealed a change in the apparent total binding of the radioligand resulting from a difference in the ability of the radioligand to discriminate the two forms of the receptor (curve  $d$  versus curve  $e$ ) than did saturation curves under identical conditions (curve  $b$  versus curve  $a$  in Fig. 3C).

scribed by  $M$ ) would also act to decrease the ability of competing ligands to stabilize the ternary complex  $HRX$  (described by  $L$ ). A gradual decrease in the over-all affinity of the competing ligand was observed with a simultaneous increase in the slope factor of the curve (due to decreasing  $L$ ) and an increase in the total binding of the radioligand (due to decreasing  $M$  toward the value of  $L$  for the radioligand; Fig. 7; Table 5; see Fig. 5B). The

TABLE 3

Parameter estimates from mass-action modeling of simulated competition curves for various competing ligands

Data were simulated<sup>a</sup> as described in Fig. 5A but with the introduction of "experimental noise" (see Appendix). Analysis was performed as described in Table 2. When the competing ligand could not discriminate the two apparent binding sites ( $L/M = 1$ ), the data were best described by only a single class of binding sites having an estimated association constant ( $K_L$ ) identical with the value of  $K$  (association constant of the competing ligand for the free form of the receptor; see Fig. 2) used in the simulations. For competing ligands having higher affinity for the free form of the receptor ( $L/M < 1$ ), the data were best described by only a single case of binding sites with an estimated association constant ( $K_L$ ) that was significantly less (lower affinity;  $p < 0.001$ ) than the value of  $K$  (curve e, Fig. 5A). For all competing ligands having higher affinity for the coupled form of the receptor ( $L/M > 1$ ), the estimated proportion of the apparent high-affinity binding site ( $\%R_H$ ) did not vary, in contrast to the ability to discriminate the two apparent binding sites ( $K_H/K_L$ ; see Fig. 6). The value of  $\%R_H$  was significantly underestimated if the analysis was conducted assuming that the radioligand did not discriminate the two forms of the receptor (parameter estimates in parentheses).

$L/M$	$K_H$ $M^{-1}$	$K_L$ $M^{-1}$	$K_H/K_L$	$\%R_H$
0.01	—	$7.1 \pm 0.2 \times 10^7$	1	0
0.1	—	$7.4 \pm 0.1 \times 10^7$	1	0
1	—	$1.0 \pm 0.2 \times 10^8$	1	0
10	$1.2 \pm 0.7 \times 10^9$ ( $8 \pm 2 \times 10^9$ )	$1.1 \pm 0.6 \times 10^8$ ( $9.0 \pm 0.6 \times 10^7$ )	$10 \pm 1$ ( $9 \pm 1$ )	$42 \pm 1$ ( $34 \pm 5$ )
100	$5 \pm 2 \times 10^9$ ( $6.3 \pm 0.9 \times 10^9$ )	$1.07 \pm 0.01 \times 10^8$ ( $9.5 \pm 0.1 \times 10^7$ )	$60 \pm 14$ ( $70 \pm 9$ )	$47.0 \pm 0.5$ ( $33.2 \pm 0.8$ )
1000	$3.7 \pm 0.3 \times 10^{10}$ ( $6.3 \pm 0.7 \times 10^{10}$ )	$1.01 \pm 0.01 \times 10^8$ ( $9.8 \pm 0.1 \times 10^7$ )	$360 \pm 31$ ( $650 \pm 65$ )	$49.0 \pm 0.6$ ( $31.9 \pm 0.9$ )

<sup>a</sup> Simulated values were  $K = 1 \times 10^8 M^{-1}$  for the competing ligand;  $K = 2 \times 10^{10} M^{-1}$ ,  $L = 0 M^{-1}$  for the radioligand;  $R = 2X = 50$  pM.

only result of further decreases in the values of these parameters was a slight but significant increase in the total binding of the radioligand as the value of  $M$  approached the value of  $L$  for the radioligand (curve d, Fig. 7).

**Effect of varying the amount of total receptor.** Another experimental manipulation that can provide insight into the nature of the interaction of the receptor and the regulatory component is the inactivation of the free receptor with irreversible ligands of the receptor or by removal of the receptor from the membrane by selective solubilization. The predictions of the model were considered in two cases: one where there were initially equal amounts of the free receptor  $R$  and the regulatory component  $X$  present and the other where the regulatory component  $X$  was initially in stoichiometrically limiting amounts ( $R = 2X$ ).

Two distinct patterns were observed in the results of the analysis of the competition simulations which could be used to assess qualitatively the relative stoichiometry of the receptor and the regulatory component (Fig. 8). In the first case, where the amounts of the receptor and the regulatory component were comparable ( $R = X$ ), a decrease in the concentration of the receptor  $R$  resulted in a gradual loss of the amount of the apparent high-affinity binding site  $R_H$  (Fig. 8A; Table 6). In contrast, in the case where the regulatory component was initially in

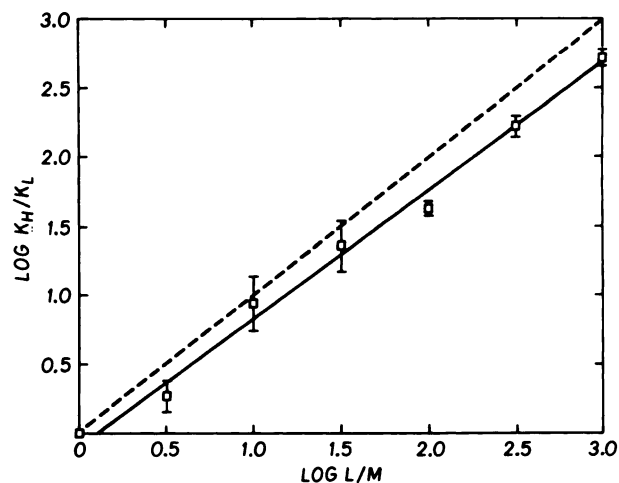


FIG. 6. Correlation of ratio of  $L/M$  (relative ability of a ligand  $H$  to stabilize the interaction of the receptor  $R$  and the regulatory component  $X$  in the form  $HRX$ ) and the ratio of estimates of the association constants ( $K_H/K_L$ ) obtained from analysis with the mass-action model

Simulations were made with a radioligand having properties similar to that in Fig. 3 (i.e., the radioligand had preferential affinity for the free form of the receptor ( $L/M \ll 1$ ) under conditions where the amount of total regulatory component  $X$  was limiting with respect to that of the receptor  $R$  ( $R = 2X$ ). Quadruplicate curves were generated and analyzed separately using the reciprocal model; each point presents the mean  $\pm$  standard error of the mean. The broken line is the line of identity, and the solid line represents the best fit to the data obtained by linear regression analysis. Although the two lines are significantly different ( $p < 0.05$  as compared with the line of identity), the results indicated that the parameter estimates obtained by analysis with the mass-action model were a good approximation of the actual ability of a ligand to stabilize the ternary complex  $HRX$ .

TABLE 4

Parameter estimates from mass-action modeling of simulated competition curves with various radioligands

Data were simulated<sup>a</sup> as described in Fig. 5B but with the introduction of "experimental noise" (see Appendix). Analysis was performed as described in Table 2. Assuming the radioligand did not discriminate the two forms of the receptor, the proportion of the apparent high-affinity binding site ( $\%R_H$ ) and the estimated ability of the competing ligand to discriminate the two apparent binding sites ( $K_H/K_L$ ) were significantly underestimated as the preference of the radioligand for the free form of the receptor increased ( $L/M \geq 0$ ).

$L/M$	$K_H$ $M^{-1}$	$K_L$ $M^{-1}$	$K_H/K_L$	$\%R_H$
0.0	$7 \pm 1 \times 10^9$	$1.01 \pm 0.3 \times 10^8$	$81 \pm 16$	$30 \pm 1$
0.1	$7 \pm 1 \times 10^9$	$1.01 \pm 0.3 \times 10^8$	$73 \pm 18$	$35 \pm 1$
0.2	$7 \pm 1 \times 10^9$	$1.01 \pm 0.3 \times 10^8$	$75 \pm 16$	$38 \pm 1$
0.5	$7 \pm 1 \times 10^9$	$1.01 \pm 0.3 \times 10^8$	$72 \pm 9$	$43 \pm 1$
1.0	$7 \pm 1 \times 10^9$	$1.01 \pm 0.3 \times 10^8$	$59 \pm 7$	$50 \pm 2$

<sup>a</sup> Simulated values were  $K = 1 \times 10^8 M^{-1}$ ,  $L = 5 \times 10^{12} M^{-1}$  for the competing ligand;  $K = 2 \times 10^{10} M^{-1}$  for the radioligand;  $R = 2X = 50$  pM.

limiting amounts ( $R = 2X$ ), a decrease in the amount of total receptor resulted in a gradual increase in the amount of  $R_H$  (Fig. 8B; Table 6).

### Experimental Data

Simulations using the ternary complex model helped to delineate several criteria necessary to be able to apply



TABLE 5

Parameter estimates from mass-action modeling of simulated competition curves with varying ability of receptor and regulatory component to interact

Data were simulated<sup>a</sup> as described in Fig. 7 but with the introduction of "experimental noise" (see Appendix). Analysis was performed as described in Table 2. With moderate decreases in the ability of the receptor and the regulatory component to interact (decreases in  $L$  for the competing ligand and of  $M$ ), the data still could be described by two apparent binding sites but with an apparent decrease in  $R$  from that determined for data generated under the initial conditions (curve  $b$ , Fig. 7). These two apparent binding sites, however, had association constants significantly different from those estimated under the initial conditions, where the decrease in the value of  $K_H/K_L$  was commensurate with the decrease in simulated value of  $L/M$ . Further decreases in both  $L$  and  $M$  resulted in a gradual loss of the apparent high-affinity site until, with low but finite values of  $L$  and  $M$ , the data could be best described by only a single class of binding sites having an association constant identical with  $K$  used in the simulations (curve  $c$ , Fig. 7). Assuming that the radioligand did not discriminate the two forms of the receptor (parameter estimates in parentheses) resulted in only a significant underestimation of the proportion of the apparent high-affinity binding site ( $\%R_H$ ) in the case of a slight ability of the receptor and the regulatory component to interact (curve  $b$ ; Fig. 7).

$M$	$L$	$K_H$	$K_L$	$\%R_H$	$K_H/K_L$
$M^{-1}$	$M^{-1}$	$M^{-1}$	$M^{-1}$		
$6 \times 10^{10}$	$1.0 \times 10^{13}$	$5.8 \pm 0.7 \times 10^9$ ( $8.0 \pm 0.8 \times 10^9$ )	$9.8 \pm 0.1 \times 10^7$	$51 \pm 1$ ( $33 \pm 1$ )	$59 \pm 7$ ( $82 \pm 9$ )
$2 \times 10^{10}$	$3.3 \times 10^{11}$	$8 \pm 1 \times 10^8$ ( $9 \pm 2 \times 10^8$ )	$1.10 \pm 0.01 \times 10^8$	$44 \pm 2$ ( $34 \pm 3$ )	$7 \pm 1$ ( $9 \pm 1$ )
$6 \times 10^9$	$1.0 \times 10^{10}$	—	$1.10 \pm 0.02 \times 10^8$	—	—
0	0	—	$9.90 \pm 0.01 \times 10^8$	—	—

<sup>a</sup> Simulated values were  $K = 1 \times 10^8 M^{-1}$  for the competing ligand;  $K = 2 \times 10^{10} M^{-1}$ ,  $L = 0 M^{-1}$  for the radioligand;  $R = 2X = 50 pM$ .

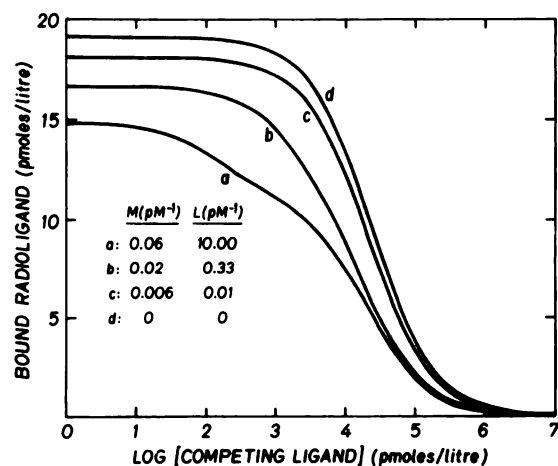


FIG. 7. Simulation of competition curves using the general form of the ternary complex model showing the effect of decreasing the interaction of the receptor  $R$  and the regulatory component  $X$ .

The radioligand was chosen initially to have lower affinity for the coupled form of the receptor ( $L/M \ll 1$ ); the competing ligand had higher affinity for the coupled form of the receptor ( $L/M > 1$ ) under conditions where the amount of the regulatory component  $X$  was less than that of the receptor  $R$  ( $R = 2X$ ; similar results were observed with  $R = X$ ). The simulations were considered as an illustration of the effect of increasing concentrations of a guanine nucleotide on the binding characteristics. The curves were simulated by a progressive reduction in the ability of the competing ligand to stabilize the ternary complex (reduction in  $L$ ) by a factor that was about 10-fold greater than that for a simultaneous reduction in the ability of the receptor  $R$  to interact spontaneously with the regulatory component  $X$  (reduction in  $M$ ). As  $L$  and  $M$  were reduced, there was a gradual decrease in the over-all potency of the competing ligand with a increase in the steepness of the curve and an increase in the total binding of the radioligand (see Table 5).

this model to ligand interactions with the pituitary dopamine receptor. Definitive testing of the model required direct curve fitting of the experimental data, utilizing the features learned from the simulations.

### Antagonist Saturation Curves

**Analysis with the mass-action model.** The representative experiment presented in Fig. 9 demonstrates that binding of the dopaminergic antagonist, [ $^3H$ ]spiperone, in membrane homogenates from bovine anterior pituitary glands was complex and affected by a guanine nucleotide (Fig. 9). In three of five membrane preparations, data obtained in the absence of Gpp(NH)p (control curves) were best explained, using the mass-action model, by two apparent binding sites, with the high-affinity site having an association constant not significantly different from that of the single binding site necessary to explain the binding data obtained in the presence of 0.1 mM Gpp(NH)p (Table 7); the ratio of  $K_H/K_L$ , calculated from five experiments, was low but significant ( $K_H/K_L = 4 \pm 1$ ). The proportion of the apparent high-affinity binding site,  $R_H$ , determined for control data was about 80% of the total specific binding of the radioligand (Table 7).

**Analysis with the ternary complex model.** Saturation data using [ $^3H$ ]spiperone were best explained where  $M = 1 \pm 0.5 \times 10^{10} M^{-1}$  in the absence of Gpp(NH)p and where there was a limiting concentration of the regulatory component ( $\%X/R = 50 \pm 19$ ); this estimate of the stoichiometry of the receptor and the regulatory component was a significantly better fit of the data than in the case where the amounts of the receptor  $R$  and the regulatory component  $X$  were constrained to be equal ( $p < 0.001$ ). These results imply that essentially all of the regulatory component was coupled in the form  $RX$  or that as much as 50% of the receptor was found in this coupled form, in the absence of the radioligand. In the absence of Gpp(NH)p it was not possible to estimate a finite value of  $L$  for [ $^3H$ ]spiperone, implying that this antagonist was binding predominantly to the free form of the receptor. It was noted that the estimate of  $K$  (association constant for the free form of the receptor,  $R$ ) was in excellent agreement with  $K_H$  for [ $^3H$ ]spiperone

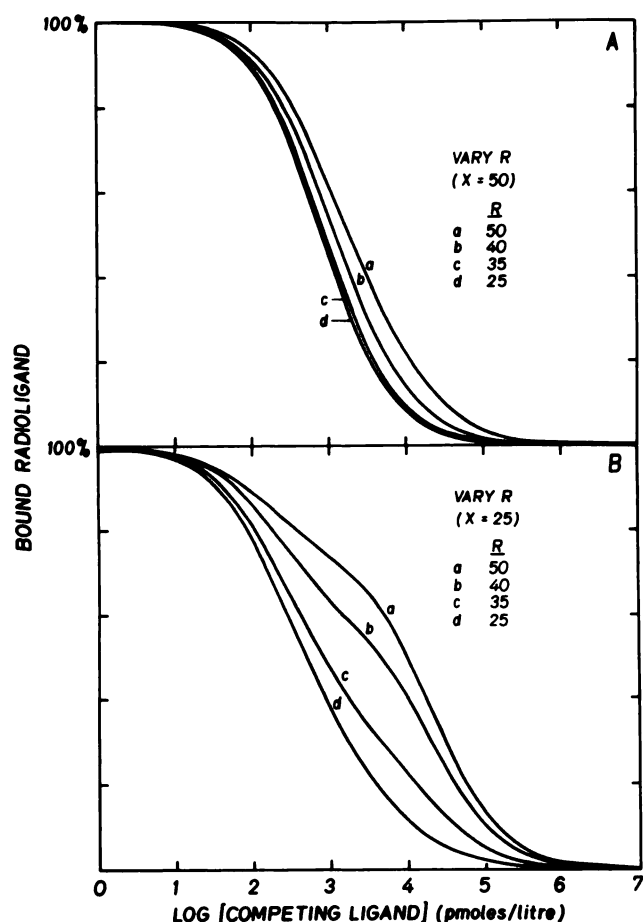


FIG. 8. Simulation of competition curves using the general form of the ternary complex model showing the effect of reducing the amount of total receptor  $R$ .

Competition curves were generated by considering a radioligand having preferential affinity for the free form of the receptor  $R$  ( $L/M \ll 1$ ) and a competing ligand having higher affinity for the coupled form of the receptor  $RX$  ( $L/M > 1$ ). A. Normalized curves in the case where the amounts of the receptor  $R$  and the regulatory component  $X$  were initially equal. B. Normalized curves in the case where initially the amount of the regulatory component  $x$  was limiting ( $R = 2X$ ). Analysis of the results demonstrate that distinct patterns are observed as the amount of the receptor is decreased depending on the initial stoichiometry of the receptor and the regulatory component (see Table 6).

in control curves and for the binding of [ $^3\text{H}$ ]spiperone in the presence of an excess of Gpp(NH)p determined by the mass-action model.

#### Agonist/[ $^3\text{H}$ ]Spiperone Competition Curves

**Analysis with the mass-action model.** Agonist/[ $^3\text{H}$ ]spiperone competition curves were "shallow" (slope factors ranged from 0.62 to 0.74), and for the three agonists studied the data were best described by the mass-action model with two apparent binding sites. Each apparent binding site had reciprocal affinity for the competing ligand and the radioligand, and in all cases the proportions of these two apparent binding sites were not significantly different from 50% (Fig. 10; Table 8). The three agonists were observed to discriminate significantly, to varying degrees, these two binding sites, with values of  $K_H/K_L$  ranging from  $46 \pm 6$  for NPA to  $200 \pm$

TABLE 6

Parameter estimates from mass-action modeling of simulated competition curves in the case where the amount of the receptor was varied

Data were simulated\* as described in Fig. 8 but with the introduction of "experimental noise" (see Appendix). Analysis was performed as described in Table 2. The major effects observed in competition curves when the amount of total receptor  $R$  was decreased below that of the regulatory component  $X$  was a gradual loss of the absolute amount of the apparent high-affinity binding site ( $R_H$ ) with no significant effect on the absolute amount of the apparent low-affinity binding site ( $R_L$ ) and an increase in the value of  $K_L$  without any effect on  $K_H$  (Fig. 8A). In the case where the regulatory component was initially in stoichiometrically limiting amounts, the major result of decreasing  $R$  toward  $X$  was a gradual decrease in the absolute amount of the apparent low-affinity binding site ( $R_L$ ) with no effect on the absolute value of the apparent high-affinity binding site ( $R_H$ ), and a slight but significant increase in  $K_L$  with no effect on  $K_H$  (Fig. 8B). Under this condition, the net effect was thus a marked apparent increase in  $R_H$ , significantly affecting the shape of the curve.

X = 50						
R	%RX	$K_H$	$K_L$	$K_H/K_L$	$R_L$	% $R_H$
		$M^{-1}$	$M^{-1}$			
50	57	$1.23 \pm 0.03 \times 10^{10}$	$7.7 \pm 0.1 \times 10^8$	16	12	$77 \pm 0.2$
40	61	$1.87 \pm 0.09 \times 10^{10}$	$3.4 \pm 0.1 \times 10^8$	5	11	$73 \pm 1$
30	65	$1.37 \pm 0.02 \times 10^{10}$	$6.2 \pm 0.3 \times 10^8$	2	7	$77 \pm 0.1$
25	67	$1.30 \pm 0.01 \times 10^{10}$	$7.7 \pm 0.1 \times 10^8$	1.7	5	$80 \pm 0.1$

X = 25						
R	%RX	$K_H$	$K_L$	$K_H/K_L$	$R_H$	% $R_L$
		$M^{-1}$	$M^{-1}$			
50	33	$7.3 \pm 0.9 \times 10^9$	$9.8 \pm 0.1 \times 10^7$	75	25	$49 \pm 0.1$
40	38	$6.0 \pm 0.6 \times 10^9$	$1.03 \pm 0.01 \times 10^8$	58	25	$38 \pm 0.1$
30	42	$5.5 \pm 0.4 \times 10^9$	$1.13 \pm 0.08 \times 10^8$	49	24	$19 \pm 0.1$
25	45	$5.4 \pm 0.6 \times 10^9$	$2.5 \pm 0.3 \times 10^8$	22	22	$13 \pm 0.2$

\* Simulated values were  $K = 1 \times 10^8 M^{-1}$ ,  $L = 5 \times 10^{12} M^{-1}$  for the competing ligand;  $K = 2 \times 10^{10} M^{-1}$ ,  $L = 0 M^{-1}$  for the radioligand;  $M = 6 \times 10^{10} M^{-1}$ ,  $R = 50 \text{ pM}$ .

130 for ADTN ( $p < 0.05$ , Student's  $t$ -test). Data obtained in the presence of 0.1 mM Gpp(NH)p were typically "right-shifted" (lower agonist affinity) and "up-shifted" (higher total binding of the radioligand) with a significant increase in the slope factor of the curve (slope factor = 0.86–0.95). In all experiments using either apomorphine or ADTN, data obtained in the presence of Gpp(NH)p were best described by the mass-action model as consisting of a homogenous population of binding sites. With apomorphine, the association constant determined in the presence of the guanine nucleotide was not significantly different from that for the low-affinity binding site estimated in the control experiments ( $K_L = 1.4 \pm 0.15 \times 10^6 M^{-1}$  and  $K_{PNP} = 1.00 \pm 0.01 \times 10^6 M^{-1}$ ;  $p > 0.5$ ). With ADTN, however, these two parameter estimates appeared to be significantly different ( $K_L = 5.9 \pm 0.83 \times 10^7 M^{-1}$ ;  $K_{PNP} = 3.6 \pm 0.26 \times 10^7 M^{-1}$ ;  $p < 0.001$ ). In contrast, with two of three experiments using NPA, a small, but significant, proportion of an apparent high-affinity binding site ( $14 \pm 7\%$  of total binding) was observed in the presence of Gpp(NH)p, having an association constant identical with the apparent high-affinity binding site of control curves ( $3 \pm 2 \times 10^{10} M^{-1}$ ); as well, with all experiments using NPA, the association constant of the apparent low-affinity binding site observed in the presence of the guanine nucleotide was significantly of



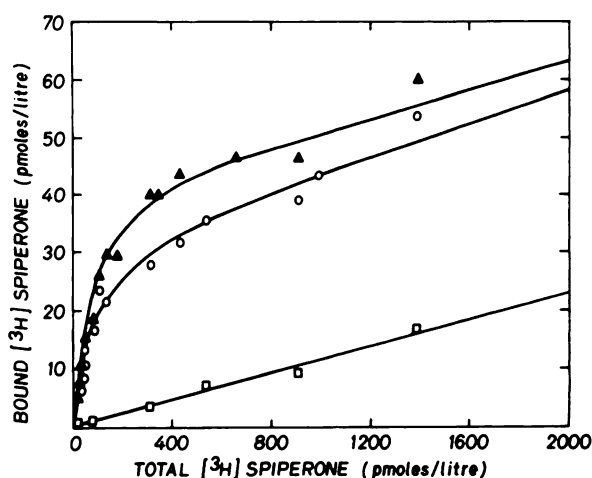


FIG. 9. Representative saturation curve of [ $^3\text{H}$ ]spiperone in bovine anterior pituitary membranes

Bound radioactivity at increasing concentrations of [ $^3\text{H}$ ]spiperone (10–1500 pM) was measured in the absence (○) and presence (▲) of 0.1 mM Gpp(NH)p and in the presence of 5  $\mu\text{M}$  (+)-butaclamol [nonspecific binding (□)]. There was no effect of Gpp(NH)p on the nonspecific binding. The lines represent the best fit of the data with the ternary complex model when the two curves were analyzed simultaneously to share receptor capacity and estimates for  $K$  (association constant of ligand for the free form of the receptor  $R$ ). Preliminary analysis with the ternary complex model of data obtained in the presence of Gpp(NH)p revealed that it was impossible to estimate a finite value of  $L$  for the radioligand (association constant for the free form of the receptor,  $R$ ), the value of  $M$  (association constant describing the interaction of the receptor with the regulatory component), and the stoichiometry of the regulatory component. As well, it was impossible to estimate a finite value of  $L$  for the radioligand in the control curves. For all four parameters, low values (not incompatible with a value of 0) were adequate, so that consequently, in all further analyses, these parameters were set to be 0. Parameter estimates for these data were as follows:  $R = 44 \pm 2$  pM;  $X = 12 \pm 3$  pM;  $K = 1.6 \pm 0.2 \times 10^{10} \text{ M}^{-1}$ ;  $L$  ( $\pm$  Gpp(NH)p) = 0  $\text{M}^{-1}$ ;  $M$  (in the absence of Gpp(NH)p) =  $1 \pm 1 \times 10^{12} \text{ M}^{-1}$ ;  $M$  (in the presence of Gpp(NH)p) = 0  $\text{M}^{-1}$ .

TABLE 7

Summary of analysis of [ $^3\text{H}$ ]spiperone binding in bovine anterior pituitary membranes

Numbers in parentheses are parameter estimates obtained for binding in the presence of 0.1 mM Gpp(NH)p. All values are the averages of five experiments.

Mass action model			
$K_H$	$K_L$	$K_H/K_L$	% $R_H$
$\text{M}^{-1}$	$\text{M}^{-1}$		
$1.6 \pm 0.2 \times 10^{10}$	$4 \pm 1 \times 10^9$	$4 \pm 1$	$78 \pm 7$
( $1.6 \pm 0.2 \times 10^{10}$ )	—	(0)	(0)
Ternary complex model			
$K$	$M$	$R$	% $X/R$
$\text{M}^{-1}$	$\text{M}^{-1}$	pM	
$1.5 \pm 0.1 \times 10^{10}$	$1 \pm 0.5 \times 10^{12}$	$50 \pm 4$	$50 \pm 19$

lower affinity as compared with  $K_L$  of the control curves ( $K_L = 1.2 \pm 0.24 \times 10^7 \text{ M}^{-1}$  and  $K_{\text{PNP}} = 4.8 \pm 0.71 \times 10^7 \text{ M}^{-1}$ ;  $p < 0.001$ ).

**Analysis with the ternary complex model.** Independent analysis with each of the three agonists provided identical estimates for those parameters describing the inter-

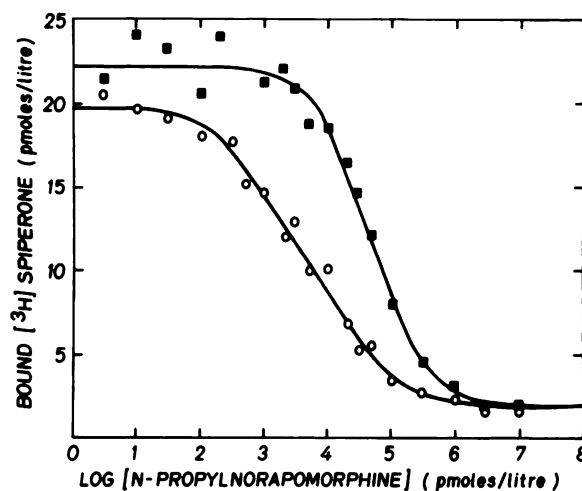


FIG. 10. Representative competition curve for increasing concentrations of NPA with 100 pM [ $^3\text{H}$ ]spiperone in the absence (○) and presence (■) of 0.1 mM Gpp(NH)p

The lines represent the best fit of the data with the ternary complex model when the two curves were analyzed simultaneously to share receptor capacity and  $K$  (association constant of ligand for the free form of the receptor  $R$ ) for NPA. Analysis with the ternary complex model was conducted assuming that the value of  $K$  for [ $^3\text{H}$ ]spiperone (association constant for the free form of the receptor  $R$ ) was  $1.6 \times 10^{10} \text{ M}^{-1}$  and that its value of  $L$ , in the presence and absence of Gpp(NH)p, was 0 (i.e., that it bound predominantly to the free form of the receptor  $R$ ) (see Table 8). As was observed when attempting to fit the ternary complex model to saturation curves of [ $^3\text{H}$ ]spiperone performed in the presence of the guanine nucleotide, in the seven of nine competition experiments where only a single apparent binding site was observed in the presence of Gpp(NH)p, there was no information regarding the interaction of the receptor with the regulatory component. A value for  $M$  of 0 was compatible and was set constant as such in all further analyses. Simultaneous analysis of data obtained in the presence and absence of 0.1 mM Gpp(NH)p was conducted, sharing the value of  $K$  (association constant for the free form of the receptor) and the value of  $R$  between the two curves. Parameter estimates for these data, obtained assuming that  $K = 1.6 \times 10^{10} \text{ M}^{-1}$  and  $L = 0 \text{ M}^{-1}$  for the radioligand, were as follows:  $R = 44 \pm 2$  pM;  $X = 34 \pm 3$  pM;  $K_{\text{NPA}} = 5.8 \pm 0.7 \times 10^7 \text{ M}^{-1}$ ;  $L_{\text{NPA}} = 1.2 \pm 0.5 \times 10^{12} \text{ M}^{-1}$ ;  $M = 1.4 \pm 0.7 \times 10^{10} \text{ M}^{-1}$ .

action between the receptor and the regulatory component (Table 8); an average estimate of  $M = 1.6 \pm 0.13 \times 10^{10} \text{ M}^{-1}$  (association constant of the receptor  $R$  with the regulatory component  $X$ ) was determined, with an average of the stoichiometric ratio of the receptor and the regulatory component estimated to be  $X/R = 56 \pm 2.3\%$ . This estimate of  $X/R$  was a significantly better fit of the data as compared with the case where the amounts of the receptor  $R$  and the regulatory component  $X$  were constrained to be equal ( $p < 0.001$ ). These results imply that in the absence of any ligand approximately 40% of the receptor pool is coupled to a regulatory component or that about 80% of the regulatory component pool is in association with a receptor. The values of these parameter estimates are considerably less than those determined in the analysis of the saturation data of the antagonist, [ $^3\text{H}$ ]spiperone. We conclude, however, that the values obtained from the analysis of competition data are more precise parameter estimates, since the simultaneous analysis of competition data obtained in

TABLE 8

*Parameter estimates from analysis of competition data in bovine anterior pituitary membranes*

Analysis of agonist/[<sup>3</sup>H]spiperone curves, performed using any particular membrane preparation, was conducted usually utilizing parameter estimates for the radioligand obtained from saturation analysis of [<sup>3</sup>H]spiperone in the same membrane preparation by methods described in text. In all competition experiments, the total binding of the single low concentration of [<sup>3</sup>H]spiperone (in the absence of competing ligand) was significantly higher in the presence of Gpp(NH)p than in its absence (see Fig. 10). For this reason, simultaneous analysis of data obtained in the presence and absence of the guanine nucleotide was used to provide a parameter estimate of  $K_L$  for the radioligand, when using the mass-action model. This procedure routinely gave a much better fit of the mass-action model to the experimental data, even in those cases where previous estimates of  $K_L$  for the radioligand were not well determined. It was usually much easier to detect this effect of the nucleotide on the binding of [<sup>3</sup>H]spiperone when using competition curves than with saturation analysis, since the latter approach must rely on the upper range of experimental data, where the experimental error is usually quite high.

Mass-action model <sup>a</sup>					
Ligand	Slope	$K_H$ $M^{-1}$	$K_L$ $M^{-1}$	$K_H/K_L$	% $R_H$
NPA	$0.62 \pm 0.05$ ( $0.86 \pm 0.07$ )	$5 \pm 1 \times 10^9$ (—)	$1.2 \pm 0.2 \times 10^8$ ( $5.5 \pm 0.7 \times 10^7$ )	$46 \pm 6$	$59 \pm 3$
Apomorphine	$0.71 \pm 0.02$ ( $0.89 \pm 0.03$ )	$1.0 \pm 0.4 \times 10^9$ (—)	$1.4 \pm 0.2 \times 10^7$ ( $1.0 \pm 0.1 \times 10^7$ )	$70 \pm 20$	$44 \pm 3$
ADTN	$0.74 \pm 0.02$ ( $0.95 \pm 0.05$ )	$1.3 \pm 0.9 \times 10^9$ (—)	$5.9 \pm 0.8 \times 10^6$ ( $3.6 \pm 0.3 \times 10^6$ )	$200 \pm 130$	$39 \pm 5$
Ternary complex model					
Ligand	$L$ $M^{-1}$	$K$ $M^{-1}$	$M$ $M^{-1}$	$L/M$	% $X/R$
NPA	$2.7 \pm 0.8$	$5.8 \pm 0.2 \times 10^7$	$1.7 \pm 0.2 \times 10^{10}$	$150 \pm 40$	$60 \pm 11$
Apomorphine	$5 \pm 2$	$1.1 \pm 0.01 \times 10^7$	$1.7 \pm 0.4 \times 10^{10}$	$260 \pm 80$	$52 \pm 9$
ADTN	$0.8 \pm 0.1$	$3.2 \pm 0.2 \times 10^6$	$1.3 \pm 0.2 \times 10^{10}$	$67 \pm 5$	$67 \pm 5$

<sup>a</sup> SLOPE refers to the slope factor of the curve determined by non-linear regression analysis. Numbers in parentheses are the parameter estimates for the association constants of the ligand to the single class of binding sites observed in the presence of 0.1 mM Gpp(NH)p. Analysis was conducted assuming parameter estimates for [<sup>3</sup>H]spiperone as presented in Table 7. All values are the means of three experiments.

the presence and absence of the guanine nucleotide also provides a better estimate of the discrimination of the two forms of the receptor. Estimates of the value of  $L$  (constant describing the ligand-induced association of the receptor and the regulatory component) differed significantly between each agonist, ranging from  $5 \pm 2.1 \times 10^{12} M^{-1}$  for apomorphine to  $0.8 \pm 0.12 \times 10^{12} M^{-1}$  for ADTN ( $p < 0.01$ ; Student's  $t$ -test). This trend for the estimated ratio of  $L/M$  for each agonist is reciprocal to that estimated for  $K_H K_L$  from the mass-action model (Table 8). Analysis of competition data with NPA in the cases where an apparent high-affinity binding site was detectable in the presence of Gpp(NH)p suggested a model assuming that the amount of total regulatory component was decreased in the presence of the nucleotide, with no effect on either  $L$  for the competing ligand or  $M$  (data not shown). The interpretation of this result is not immediately clear at this time.

## DISCUSSION

**Properties of the ternary complex model.** Several properties of the model provide predictions that are easily experimentally testable. (a) The existence of an effect of guanine nucleotides on the binding of ligands suggests that this model may be appropriate to use as a first simple working model such that the receptor may interact with a guanine nucleotide-binding protein; the quality

of the effect of the guanine nucleotide may indicate whether a particular ligand has higher affinity for either the free form or the coupled form of the receptor. (b) The nature of the interaction of the receptor with the regulatory component can be examined by varying the relative concentrations of these two components in the membrane or by performing competition experiments with a radiolabeled antagonist and various competing ligands in the presence and absence of various concentrations of a guanine nucleotide. Of course, definitive testing of any model can only be made by its direct application to the experimental data.

The widespread use of models based on independent classes of binding sites to analyze ligand-binding data has necessitated a comparison of parameters between such a model and the ternary complex model. (a) In the absence of an interaction between the receptor and the regulatory component, such as is proposed to occur in the presence of an excess of a guanine nucleotide where generally only a single class of binding sites is detectable, the value of this single association constant as determined with the mass-action model is a direct measurement of the affinity of the competing ligand for the free form of the receptor. (b) Serious errors in both parameter estimation with the mass-action model and in mechanistic interpretation can be made when normalizing competition data, particularly if the total binding of single

low concentrations of the radioligand is significantly affected by a guanine nucleotide; the discrimination of the two forms of the receptor by the radioligand is always more consistent at low concentrations of the radioligand. (c) Only in the case where the amount of the regulatory component is less than that of the receptor is an estimate of the association constant for the apparent low-affinity binding site of a competition curve a good estimate of the affinity of the competing ligand for the free form of the receptor. (d) All parameter estimates pertaining to the apparent high-affinity binding site of a competition curve do not directly refer to the interaction of the competing ligand with the coupled form of the receptor; the only exception to this is the estimation of functional stoichiometry of the receptor and the regulatory component, and then only when the amount of the regulatory component is limiting. (e) The value of the ratio of the association constants of the two apparent binding sites of a competition curve ( $K_H/K_L$ ) is a good estimate of the ability of the competing ligand to stabilize the association of the receptor and the regulatory component in the form of the ternary complex ( $L/M$ ). At least for the *beta*-adrenergic receptor of the frog erythrocyte, there appears to be a good correlation of this ratio and the intrinsic activity of the particular ligand in its effector system (4); use of this ratio as a measure of the "sensitivity" of the receptor system is advocated over that of the proportion of the apparent high-affinity binding site, as the former value is independent of the functional stoichiometry of the receptor and the regulatory component as modeled by the ternary complex model.

**Experimental results.** The ternary complex model appears to be quite adequate in describing many of the properties of ligand binding data for the  $D_2$ -dopamine receptor in the anterior pituitary gland. In application of the mechanistically more appropriate ternary complex model, we have found that our previously proposed "reciprocal model" of the receptor can be accounted for by the ternary complex model such that antagonists would bind predominantly to the free form of the receptor whereas agonists appear to have higher affinity for the coupled form of the receptor. Thus, assuming a ternary complex model, the apparent low-affinity binding site required to fit adequately the saturation data of [ $^3H$ ] spiperone with the mass-action model would now be more likely a reflection of the destabilization of the "precoupled" receptor pool, as the antagonist binds to the free receptor pool and shifts the equilibrium of the total receptor pool toward the free receptor pool.

The ternary complex model predicts other properties of the  $D_2$ -dopamine receptor that we and others have reported previously. Experimental manipulations utilizing heat or NEM result in a complete loss of agonist high-affinity binding (5, 17) and an enhancement of the binding of [ $^3H$ ]spiperone (5), as predicted by the ternary complex model. The effect of NEM was slightly more complete than the apparently analogous effect of guanine nucleotides (5), suggesting, under the assumption that NEM completely eliminates interaction of the receptor and the regulatory component, that even in the presence

of an excess of a guanine nucleotide there might still exist a small pool of coupled receptors.

At the present time, the ternary complex model is the simplest account for the interactions of ligands with receptor systems that either stimulate or inhibit adenylate cyclase activity. The few, notable differences in the application of the ternary complex model to these two receptors may be reflections of differences in the molecular mechanisms of these two physiologically contrasting systems. Most obvious is the difference in the ability of antagonists to discriminate between the two forms of the receptor. The ternary complex model can adequately explain these properties by assuming that antagonists, instead of passively occupying the binding site, actively dissociate the receptor from the regulatory component; this action is speculated to inactivate the receptor system, preventing agonists from exerting their effect. The concept of antagonist and agonist forms of the receptor is not a precedent in receptor theory. Such a dual receptor concept was proposed to account for the different properties of agonist and antagonist-binding data (18). The earlier formulation of the allosteric model, however, did not predict the current observations. Our "reciprocal model," as described with the ternary complex model, provides the basis for discrimination of different receptor forms by agonists and antagonists and, more important, predicts the experimental data. The significance of an active role of antagonists in receptor mechanisms still remains to be explored.

Although varying proportions of the apparent high-affinity state ( $R_H$ ) were observed with different agonists of the *beta*-adrenergic receptor (1), the same proportion of  $R_H$  (50%) was noted with agonists of the  $D_2$ -dopamine receptor. This difference is accounted for by the ternary complex model in as much as there are stoichiometrically similar amounts of the *beta*-adrenergic receptor and its regulatory component (4), whereas for the dopamine receptor it seems that its concentration is almost double that of its regulatory component. This justifies our earlier proposal (1) that the total receptor concentration determined by direct agonist binding is only 50% of that determined by direct antagonist binding, since only the coupled form of the receptor would be detected by the agonist in a binding assay.

The present form of the ternary complex model does not predict the existence of a receptor pool having high affinity for agonists in the presence of an excess of a guanine nucleotide. Grigoriadis and Seeman (19) have suggested that complete conversion with a guanine nucleotide is observed only in the presence of high concentrations of  $Na^+$ . Such an interpretation cannot account for our observations, since our studies were performed in the presence of 100 mM NaCl. The observation of a guanine nucleotide-resistant population of receptors has been made in this study and in others of inhibitory receptor systems, including brain dopamine receptors (16) and cardiac muscarinic cholinergic receptors (15). In the analysis of data with "incomplete conversion" by guanine nucleotides (this study) or of data obtained with the use of submaximal concentrations of a guanine nucleotide to demonstrate the interconvertibility of the two



apparent states of the *beta*-adrenergic receptor (4), the data could be adequately fit by the ternary complex model only if it was assumed that in the presence of guanine nucleotides the stoichiometry of the regulatory component was reduced. As we have also presented, there is a predicted positive correlation between  $K_H/K_L$  and  $L/M$  determined for a ligand with the mass-action model and the ternary complex model, respectively. Indeed, such a correlation exists for the *beta*-adrenergic receptor (3, 4), but this trend appears to be reversed with the present data for the  $D_2$ -dopamine receptor. A similar, related negative correlation has also been noted by Wells and collaborators (20, 21) in their study of the muscarinic cholinergic receptor system and by Hoffman *et al.* (13) in their study of the platelet *alpha*-adrenergic receptor; both of these systems also inhibit adenylate cyclase activity. As suggested by Wells (21), the nature of this correlation might be a relevant reflection of mechanistic differences between stimulatory and inhibitory receptor systems.

These results have justified an acknowledgement that the model in its present form might be too simple and that we must look for an extension or modification. The most obvious modification is to consider the identity of  $X$  in our model, to incorporate some of the recent advancements in our understanding of these regulatory components. While the heterodimeric structure described for the stimulatory regulatory component ( $N_s$ ) has also been determined for the regulatory component associated with inhibitory receptor systems ( $N_i$ ) (22, 23), there has yet to be any evidence demonstrating that the  $\alpha$ -subunit of  $N_i$  interacts directly with the catalytic subunit of adenylate cyclase. Indeed, as proposed by Northup *et al.* (22), the possible mechanism of inhibitory receptor systems might be to increase the membrane concentration of the free  $\beta$ -subunit that can be shared between  $N_s$  and  $N_i$  and to shift the equilibrium toward the reassociated  $\alpha\cdot\beta$  dimer. The significance of these results is in the complexity of interactions that may occur with the various receptor systems.

The present version of the ternary complex model can serve as a first working model, providing testable hypotheses; as we have demonstrated, it is possible to obtain some information pertaining to this model by using equations based on independent classes of binding sites. It does not, however, explicitly consider the interaction of guanine nucleotides with the regulatory component nor does it allow for the possible significance of the heterodimeric structure of the regulatory component and its ability to dissociate. It is possible to incorporate these features within the model, allowing for all of the possible interactions of the various components of the system. Our preliminary findings of such an expanded model have indicated that it might predict the occurrence of residual, high-affinity agonist binding in the presence of an excess of guanine nucleotide.<sup>2</sup> We are currently investigating experimentally testable aspects of such a model.

<sup>2</sup> A. De Léan and K. A. Wreggett, manuscript in preparation.

## ACKNOWLEDGMENT

We are grateful to Michel Blanchard for his assistance in the preparation of the manuscript.

## APPENDIX

**Data analysis.** Saturation and competition binding data were analyzed by a nonlinear, least-squares iterative procedure based on the algorithm of Marquardt and Levenberg (24) and using programs written by the senior author in PL/1 for a PDP 11/34 computer. All experimental data were expressed in terms of the concentration of radioligand bound as a function of the total concentration of varying ligand and analyzed without any transformation; the total concentration of radioligand was also included in analysis of competition data. In the case of competition curves, data were first analyzed according to a four-parameter logistic equation in order to determine the slope factor of the curve (25). All data were then analyzed using a generalized model for complex ligand-receptor systems according to the law of mass action (26, 27) by considering a model with two apparent binding sites having reciprocal affinity for agonists and antagonists (Fig. 1). These two binding sites ( $R_H$  and  $R_L$ ) were distinguished by their respective association constants,  $K_H$  and  $K_L$ . This model is referred to as the mass-action model. It is implicit in the analysis of individual curves with the mass-action model that the proportions of all binding sites are constant and independent of each other and of the presence of ligand. When using this model to analyze more than one curve, the proportions of the binding sites are allowed to vary between curves. In a system where these proportions vary with different ligands or where modulators such as guanine nucleotides appear to alter the proportions of these binding sites, then this mass-action model cannot be considered to be of mechanistic value; hence, all estimates obtained are not direct measurements of any thermodynamic parameters but are merely reflections of inherent properties of the system. For our purposes, the mass-action model was used to provide a first step in the quantitative assessment of the binding properties of the ligands.

Further analysis was conducted using equations based on an equilibrium model describing a reversible interaction of the receptor  $R$  with a regulatory component  $X$  (4, 27); the model does not explicitly consider the interaction of guanine nucleotides with the regulatory component  $X$ . This model, which we refer to as the ternary complex model, incorporates several important parameters that are summarized in Fig. 2. A general description of this model has been presented previously (4).

When using either model, data from individual experiments, obtained in the presence and absence of Gpp(NH)p, were analyzed simultaneously to enable statistical considerations of the sharing of certain parameters between the two curves. Testing for statistical significance of these constraints or for the introduction of further parameters in the analysis was conducted using a partial  $F$ -test, which compared the residual variance before and after the parameter introduction (26, 27). Increasing the complexity of a model by increasing the number of parameters will always improve the fit of the

model to the data; the statistical approach utilized here objectively ensures the simplest model by determining the point at which the relationship of the decrease in the variance and of the degrees of freedom is no longer significant. In all curve-fitting procedures the data were weighted according to the reciprocal of the predicted variance, which, in turn, was determined by use of a power function relationship between the variance and the mean; the weighting coefficients were estimated for individual curves in a preliminary analysis of replicates (28). Parameter estimates are presented as the mean  $\pm$  standard error of the mean of replicate experiments.

**Simulations of the ternary complex model.** Theoretical properties of the ternary complex model were examined by simulating ligand-binding data. Saturation curves were generated by determining the amount of bound ligand at increasing concentrations of the ligand. Competition curves were generated by determining the amount bound of a fixed concentration of a ligand (radioligand) at increasing concentrations of another ligand (competing ligand); different competing ligands and radioligands were simulated by varying the values of both  $K$  (association constant for binding to the free receptor  $R$ ) and  $L$  (equilibrium constant describing the ligand-promoted coupling of  $R$  with  $X$ ) for each ligand. In all cases where curves were analyzed using the mass-action model, data were generated to include "experimental noise" introduced by a random-number generator according to a variance function normally observed with real data (Monte Carlo simulations). Each curve included 25 points which were equidistant over 3 or 8 orders of magnitude on a logarithmic scale for saturation curves or competition curves, respectively. Replicate simulations were then analyzed, individually, using the mass-action model, as described above. Parameter estimates determined by this analysis are presented as the mean  $\pm$  standard error of the mean for three independent simulations.

**Generalized form of the ternary complex model.** In experimental systems where several ligands are competitively binding to one class of receptor sites which themselves interact with a non-receptor regulatory component, the concentration  $B_i$  of each ligand bound can be expressed as:

$$B_i = (K_i \cdot E + K_i \cdot L_i \cdot E \cdot U + N_i) \cdot F_i \quad A1$$

where  $F_i$  is the corresponding concentration of free ligand  $i$ ;  $K_i$  is the equilibrium constant of the reaction producing the binary complex  $HR_i$  of ligand  $i$  with receptor  $R$ ;  $L_i$  is the equilibrium constant of the reaction producing the ternary complex  $HRX_i$  of ligand  $i$ , receptor  $R$ , and regulatory component  $X$ ;  $N_i$  is the coefficient for nonspecific binding of ligand  $i$ ; and  $E$  and  $U$  are the concentrations of unoccupied (empty) receptors and uncoupled regulatory components, respectively. Equation A1 explicitly describes the variables  $B_i$  as a function of  $F_i$ ,  $E$  and  $U$ . However, this formulation does not directly lead to the calculation of  $B_i$ , since the variables  $F_i$  are not truly independent, being the difference  $H_i - B_i$  between the concentration of total ligand  $i$  and of bound ligand  $i$ .

By analogy with the mathematical approach used by

Feldman (29), we preferably use an implicit function of the free ligand concentration  $F_i$ :

$$G_i = H_i - F_i \cdot (1 + K_i \cdot E + K_i \cdot L_i \cdot E \cdot U + N_i) \quad A2$$

The aim of the calculation is to find for each variable  $F_i$  the value or root which satisfies  $G_i = 0$ . These values can then be used in Eq. A1 to calculate  $B_i$ , the experimentally observed variable. The variable  $E$  can be calculated from the quadratic equation:

$$T \cdot (S + 1) \cdot E^2 + (1 + S + T) \cdot (X - R) \cdot E - R = 0 \quad A3$$

where

$$S = \sum K_a \cdot F_a \\ T = M + \sum K_a \cdot L_a \cdot L_a$$

$M$  is the equilibrium constant of the reaction leading to the formation of the ligand-independent binary complex  $RX$ , and  $R$  and  $X$  are the concentrations of total receptor sites and regulatory components, respectively. The concentration of uncoupled regulatory component  $U$  is simply calculated as:

$$U = X / (1 + T \cdot E)$$

For every set of values of the model parameters  $K_i$ ,  $L_i$ ,  $N_i$ , and  $X$  and of the independent variables  $H_i$ , the variables  $F_i$  must be iteratively calculated from Eq. A2 by using a generalized Newton's method. Briefly stated, a first approximation of each  $F_i$  is obtained, then the terms  $S$  and  $T$  are calculated, and the variable  $E$  is obtained using Eq. A3, followed by the variable  $U$ . Corrections to the initial estimates for  $F_i$ , which should satisfy  $G_i = 0$ , can be obtained according to Newton's method:

$$\text{New } F_i = F_i - (A_{ii})^{-1} \cdot G_i \quad A4$$

where  $(A_{ii})^{-1}$  is the inverse matrix of  $A_{ii} = \partial G_i / \partial F_i$ . The improved estimates of  $F_i$  are then used to calculate new corrections for  $F_i$  until the results converge to stable values, usually after three to five iterations.

Finally, the independent variables  $B_i$  are calculated using Eq. A1.

In the case where the ternary complex model is used for nonlinear least-squares curve fitting, the partial derivatives of the observed variables  $B_i$  with respect to each parameter  $P$  of the model ( $K_i$ ,  $L_i$ ,  $M$ ,  $N_i$ ) can be easily obtained from:

$$\partial B_i / \partial P = (A_{ii})^{-1} \cdot (\partial G_i / \partial P) \quad A5$$

where  $A_{ii}$  has the same value as in Eq. A4 and  $\partial G_i / \partial P$  is the partial derivative of the implicit function  $G_i$  with respect to parameter  $P$ .

## REFERENCES

- De Lean, A., B. F. Kilpatrick, and M. Caron. Dopamine receptor of the porcine anterior pituitary gland: evidence for two affinity states of the receptor discriminated by both agonists and antagonists. *Mol. Pharmacol.* 22:290-297 (1982).
- Onali, P., J. P. Schwartz, and E. Costa. Dopaminergic modulation of adenylate cyclase stimulation by vasoactive intestinal peptide in anterior pituitary. *Proc. Natl. Acad. Sci. U. S. A.* 78:6531-6534 (1981).
- Kent, R. S., A. De Lean, and R. J. Lefkowitz. A quantitative analysis of  $\beta$ -adrenergic receptor interactions: resolution of high and low affinity states of

- the receptor by computer modeling of ligand binding data. *Mol. Pharmacol.* 17:14-23 (1980).
4. De Lean, A., J. M. Stadel, and R. J. Lefkowitz. A ternary complex model explains the agonist-specific binding properties of the adenylate cyclase-coupled  $\beta$ -adrenergic receptor. *J. Biol. Chem.* 255:7108-7117 (1980).
  5. Kilpatrick, B. F., A. De Lean, and M. Caron. Dopamine receptor of the porcine anterior pituitary gland: effects of *N*-ethylmaleimide and heat on ligand binding mimic the effects of guanine nucleotides. *Mol. Pharmacol.* 22:298-303 (1982).
  6. Jakobs, K. H., P. Lasch, M. Minuth, K. Aktories, and G. Schultz. Uncoupling of  $\alpha$ -adrenoceptor-mediated inhibition of human platelet adenylate cyclase by *N*-ethylmaleimide. *J. Biol. Chem.* 257:2829-2833 (1982).
  7. Roas, E. M., and A. G. Gilman. Resolution of some components of adenylate cyclase necessary for catalytic activity. *J. Biol. Chem.* 252:6966-6969 (1979).
  8. Cronin, M. J., G. A. Myers, R. M. MacLeod, and E. L. Hewlett. Pertussis toxin uncouples dopamine agonist inhibition of prolactin release. *Am. J. Physiol.* 244:E499-E504 (1983).
  9. Katada, T., and M. Ui. Slow interaction of islet-activating protein with pancreatic islets during primary culture to cause reversal of  $\alpha$ -adrenergic inhibition of insulin secretion. *J. Biol. Chem.* 255:9580-9588 (1980).
  10. Kurose, H., T. Katada, T. Amano, and M. Ui. Specific uncoupling by islet-activating protein, pertussis toxin, of negative signal transduction via  $\alpha$ -adrenergic, cholinergic, and opiate receptors in neuroblastoma  $\times$  glioma hybrid cells. *J. Biol. Chem.* 258:4870-4875 (1983).
  11. Bokoch, G. M., T. Katada, J. K. Northrup, E. L. Hewlett, and A. G. Gilman. Identification of the predominant substrate for ADP-ribosylation by islet activating protein. *J. Biol. Chem.* 258:2072-2075 (1983).
  12. Kilpatrick, B. F., and M. G. Caron. Agonist binding promotes a guanine nucleotide reversible increase in the apparent size of the bovine anterior pituitary dopamine receptors. *J. Biol. Chem.* 258:13528-13534 (1983).
  13. Hoffman, B. B., T. Michel, T. B. Brenneman, and R. J. Lefkowitz. Interactions of agonists with platelet  $\alpha$ -adrenergic receptors. *Endocrinology* 110:926-932 (1982).
  14. Sibley, D. R., A. De Lean, and I. Creese. Anterior pituitary dopamine receptors: demonstration of interconvertible high and low affinity states of the D-2 dopamine receptor. *J. Biol. Chem.* 257:6351-6361 (1982).
  15. Burgisser, E., A. De Lean, and R. J. Lefkowitz. Reciprocal modulation of agonist and antagonist binding to muscarinic cholinergic receptor by guanine nucleotides. *Proc. Natl. Acad. Sci. U. S. A.* 79:1732-1736 (1982).
  16. Wreggett, K. A., and P. Seeman. Agonist high- and low-affinity states of the D<sub>2</sub>-dopamine receptor in calf brain: partial conversion by guanine nucleotide. *Mol. Pharmacol.* 25:10-17 (1984).
  17. George, S. R., M. Watanabe, and P. Seeman. Commentary: the dopamine receptor of the anterior gland, in *Dopamine Receptors* (C. Kaiser and J. W. Kebabian, eds.). American Chemical Society, Washington, D. C., 93-99 (1983).
  18. Greenberg, D. A., D. C. U'Pritchard, and S. H. Snyder.  $\alpha$ -noradrenergic receptor binding in mammalian brain: differential labeling of agonist and antagonist states. *Life Sci.* 19:69-76 (1976).
  19. Grigoriadis, D., and P. Seeman. Sodium ions convert brain D<sub>2</sub> dopamine receptors from high to low affinity for dopamine agonists. *Soc. Neurosci. Abstr.* 9:31 (1983).
  20. Wells, J. W., H.-M. Wong, T. W. T. Lee, and M. J. Sole. Multiple states of cardiac muscarinic receptors. *Soc. Neurosci. Abstr.* 8:340 (1982).
  21. Wells, J. W. Mechanistic interpretation of radioligand binding patterns of neurohumoral receptors. *J. Neurochem. [Suppl.]* 41:S162 (1983).
  22. Northrup, J. K., P. C. Sternweis, and A. G. Gilman. The subunits of the stimulatory regulatory component of adenylate cyclase: resolution, activity, and properties of the 35,000-dalton ( $\beta$ ) subunit. *J. Biol. Chem.* 258:11361-11368 (1983).
  23. Codina, J., J. Hildebrandt, R. Iyengar, L. Birnbaumer, R. D. Sekura, and C. R. Manclark. Pertussis toxin substrate, the putative N<sub>i</sub> component of adenylate cyclases, is an  $\alpha$ - $\beta$  heterodimer regulated by guanine nucleotide and magnesium. *Proc. Natl. Acad. Sci. U. S. A.* 80:4276-4280 (1983).
  24. Magar, E. M. *Data Analysis in Biochemistry and Biophysics*. Academic Press, New York, 141-162 (1972).
  25. De Lean, A., P. J. Munson, and D. Rodbard. Simultaneous analysis of families of sigmoidal curves: application to bioassay, radioligand assay, and physiological dose-response curves. *Am. J. Physiol.* 235:E97-E102 (1978).
  26. De Lean, A., A. A. Hancock, and R. J. Lefkowitz. Validation and statistical analysis of the computer modeling method for quantitative analysis of radioligand binding data for mixtures of pharmacological receptor subtypes. *Mol. Pharmacol.* 21:5-16 (1982).
  27. De Lean, A. Computer modelling of adenylate cyclase coupled hormone receptor systems, in *Serono Symposium on Training on Computers in Endocrinology* (D. Rodbard and G. Forti, eds.). Academic Press, in press (1984).
  28. Rodbard, D., R. H. Lenox, H. L. Wray, and D. Ramseth. Statistical characterization of the random errors in the radioimmunoassay variable. *Clin. Chem.* 22:350-358 (1976).
  29. Feldman, H. A. Mathematical theory of complex ligand-binding systems at equilibrium: some methods for parameter fitting. *Anal. Biochem.* 48:317-338 (1972).

Send reprint requests to: Dr. André De Léan, Institut de Recherches Cliniques de Montréal, 110 avenue des Pins, ouest, Montréal, Québec, H2W 1R7, Canada.